CASE STUDY OF THE CHALLENGING INSTALLATION OF A TURBOPROP FLOW EVACUATION SYSTEM

Vicente Ibáñez, David Perdones** and Emilio J. Angel****
** Aerodynamics Domain*
Airbus Military
28906 Getafe, Spain
Phone: +34 91 624 4912
vicente.ibanez@military.airbus.com
*** Aerodynamics Domain*
Airbus Military
28906 Getafe, Spain
Phone: +34 91 624 7065
david.perdones@military.airbus.com
******* *Head of Aerodynamics Domain*
Airbus Military
28906 Getafe, Spain
Phone: +34 91 624 5077
emilio.angel@military.airbus.com

Abstract

The integration of the airframe and a turboprop propulsion system entails several challenges. One of them is the installation of the exhaust. If the exhaust is part of the nacelle ventilation system acting as an eductor, the equipments housed inside the engine ventilation bay have also to be protected from the effects of the exhaust hot gases.

This paper is an account of how exhaust installation challenges were approached in the A400M Aircraft. The engineering process is described. CFD codes were extensively used for the design. Ground and Flight test campaigns showed that proposed design was efficient at meeting the requirements.

1. Ventilation system description

The purpose of nacelle ventilation systems is to provide ventilation airflow through the engine bay on the ground and at low speed, keeping the nacelle equipment at suitable conditions. Further, nacelle ventilation flows reduce the risk of a nacelle fire. If there is a fuel leak, the ventilation helps to reduce the concentration of fumes.

Figure 1 describes schematically the flow evacuation system used to ensure the ventilation of the nacelle bay which houses the engine and auxiliary equipment. Ventilation flow is energized as it is mixed with the engine flow which acts as an eductor (reference 1). The eductor role is to provide entrainment of airflow coming from the nacelle bay area. In principle this system should allow for the right nacelle cooling at any flight condition without the need of dedicated ejectors using engine bleed air.

In order to identify the different sections representative of the system operation, the following Stations are defined (figure 2):

- Station 17 : Control section located at the nacelle ventilation bay.
- Station 18 : stands for the discharge section of nacelle ventilation flow on the eductor.
- Station 7: Control section located at the entry of the engine nozzle.
- Station 8: stands for the exit section of the engine nozzle.
- Station 28 : stands for the discharge section of the engine Outlet Guide Vane cooling flow; which has been previously bled from the upstream nacelle ventilation flow.
- Station 9: Exit section of the exhaust to ambient.

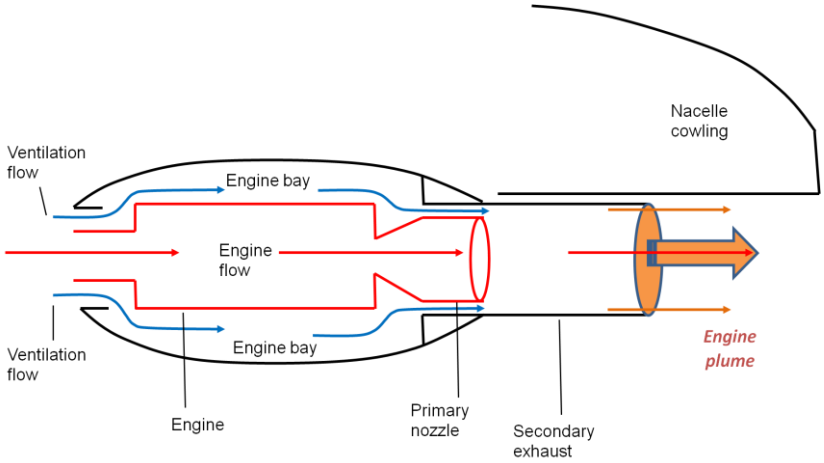

Figure 1: Eductor system operation

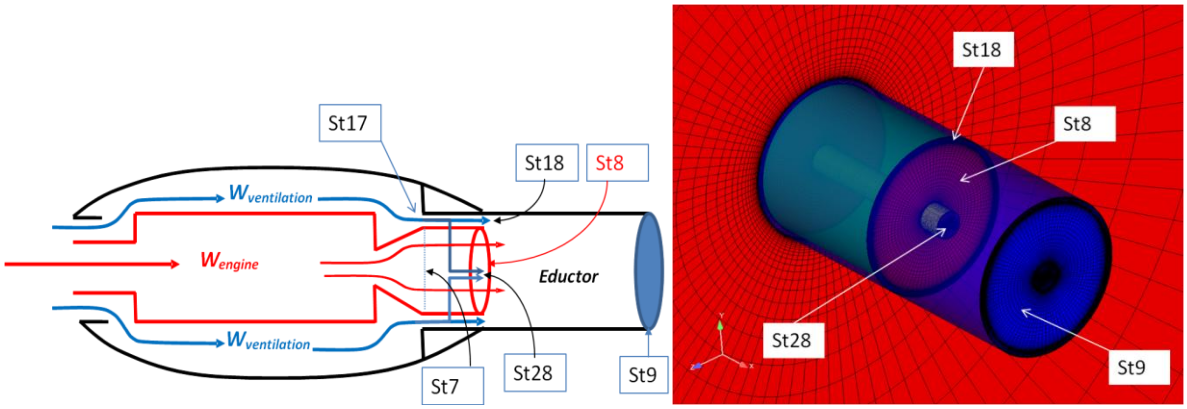

Figure 2: Axisymmetric Eductor Stations

The design verification and validation process of the ventilation system included the following steps:

1. Ground testing. The first experimental assessments of engine installation effects are done on these tests. Figure 3 show a test bench sited in Moron (Seville-Spain).
2. Flying Test Bed (FTB). It is essentially a risk reduction stage. The full PowerPlant is installed on an existing A/C. In the A400M case a C130 A/C was the supporting vehicle (figure 4).
3. A/C prototypes. The PowerPlant installation characteristics are finally checked on the actual A/C frame (figure 5).

Ground tests conducted on the ground bench and flight test conducted on FTB showed that for some conditions, particularly at low power settings, there was risk of overheating of nacelle equipments and structural components. This effect was confirmed on the A400M first prototypes.

Figure 3: Moron Test Bench.

Figure 4: Flying Test Bed.

Figure 5: A400M Aircraft

2. Identification of ventilation issue

In accordance with temperature measurements, it was identified that the reason for overheating was the hot engine exhaust flow re-ingested towards the engine ventilation bay due to the highly swirling gases of the engine at the primary nozzle at low power settings which significantly reduces the eductor effect.

2.1 Test Data

Figure 6 shows total pressure maps constructed from a total pressure rake located at the exit of the engine. The left side shows the pressure map corresponding to a typical cruise condition. The right side shows the pressure map at a ground idle condition. It can be seen that high swirling flows at idle conditions cause the separation of upstream stator wakes, whose traces are clearly visible on the right figure.

Figure 7 shows a pressure map constructed from static pressure measurements at the exit of the exhaust at a Ground Idle condition. The radial variation of static pressure is produced by engine swirling flow.

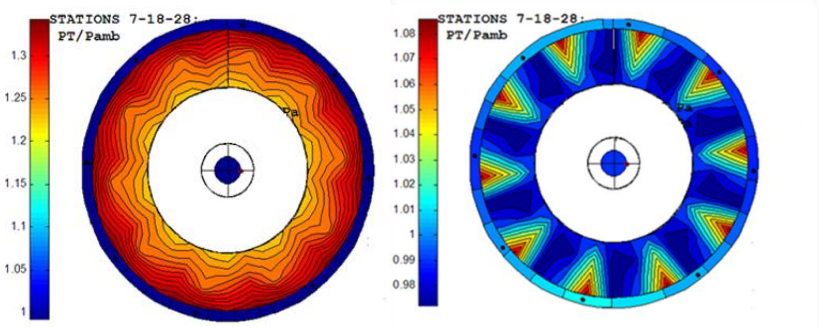

Figure 6: Total pressure measurements (cruise (left picture)-Flight Idle (right picture)).

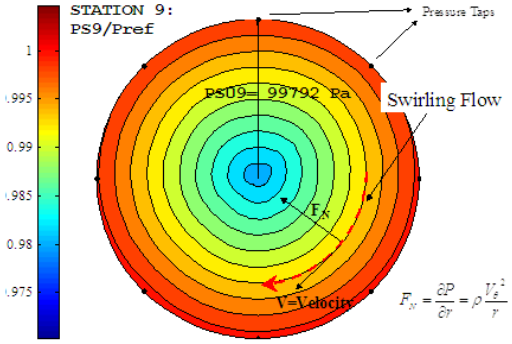

Figure 7: Static pressure measurements at the exit of the exhaust (ground idle).

As the engine flow swirl increases, the engine flow **tends to expand** towards the secondary exhaust casing by **centrifugal force**, collapsing the ventilation flow discharge (figure 8).

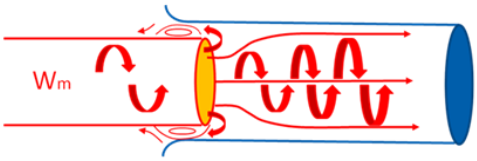

Figure 8.High swirl effect on eductor operation

2.2 CFD investigation

A simple CFD analysis was conducted to confirm the impact of the engine swirl on the eductor operation. Figure 9 shows the streamline flow pattern of an axisymmetric eductor calculated with the CFD solver Fluent (version 6.3) axisymmetric analysis module (constant engine swirl). Figure 9(left) flow pattern corresponds to a condition with engine swirl sufficiently low; while Figure 9 (right) shows how Stations 18 and 28 get blocked when the engine swirl is sufficiently high.

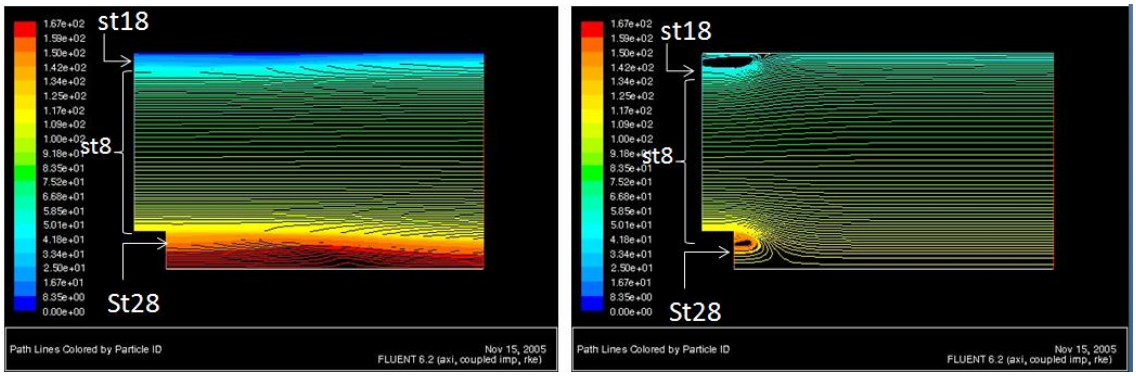

Figure 9. Eductor flow pattern. Baseline Eductor

Once confirmed the source of the flow re-ingestion and to assess the effect of installation, a full 3D model comprised of the wing, the nacelle and the exhaust was studied using the CFD code Fluent. The flight condition considered for this simulation was the most critical from the point of view of the nacelle ventilation, i.e., a low power engine regime (Ground Idle), where the engine swirl is maximum, at high ambient temperature (Sea Level, ISA+40).

Figure 10 shows the complete 3D model. The propeller effects were introduced by means of an actuator disk model with a distribution of radial pressure jump and swirl. The pressure increase was derived from the propeller deck provided by the propeller manufacturer. The engine was modeled using a mass flow boundary condition, where the engine mass flow, the total temperature and the swirl of the combustion gases are imposed. All these values were calculated with the aid of the engine deck. The boundary condition is located at the low pressure turbine exit plane, upstream of the Outlet Guide Vanes. Farfield boundary conditions were imposed by means of Riemann Boundary Conditions. It is important to note that for this simulation the radiation and heat conduction effects of the engine were taken into account.

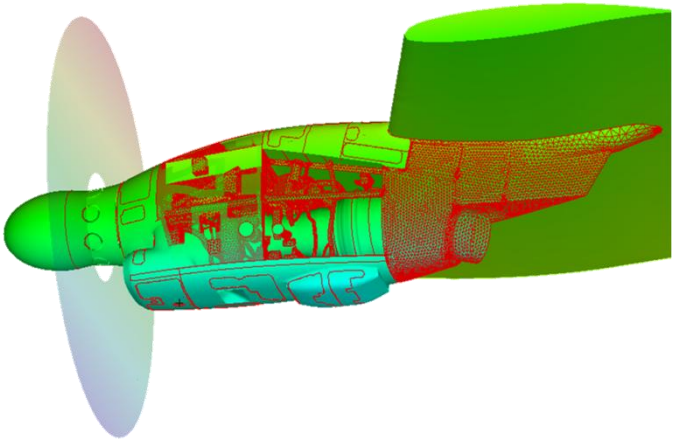

Figure 10: Computational ventilation model. CFD domain

The computational domain was meshed with a conformal tetrahedral mesh. Figure 11 shows the mesh for the engine nozzle. Except inside the nacelle ventilation bay where the velocities are very small prisms were extruded. The total mesh size is roughly $6 \cdot 10^6$ cells. The k-ω SST turbulence model was used and a second order spatial discretization scheme was used for all equations. From all the available algorithms in Fluent version 6.3 to solve the Navier-Equations, the implicit pressure based coupled was selected.

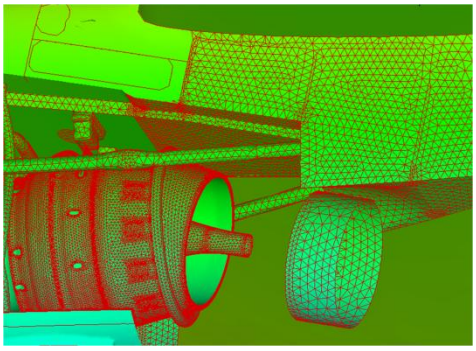

Figure 11: CFD model: mesh for engine nozzle area

The results from this CFD study confirmed that the high engine swirl was the main cause for the eductor operation failure. As it was previously envisaged from the simplified axisymmetric CFD results.

Figure 12 shows the flow separation that occurs at the Outlet Guide Vanes due to the high engine swirl. This flow pattern is consistent with that measured during flight tests shown in Figure 8 (right).

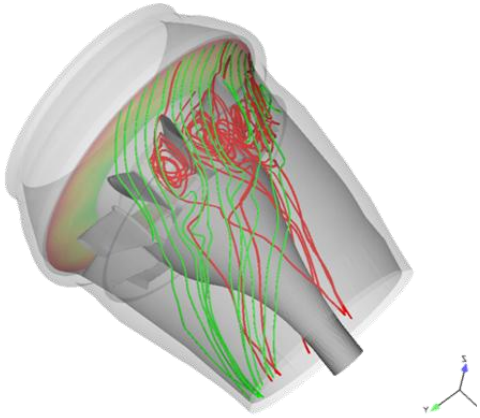

Figure 12: CFD Streamlines (engine nozzle).

Figure 13 shows velocity vectors at Station 18. As it can be seen, exhaust gases recirculate into the nacelle ventilation bay. The recirculation effect is more severe on the upper side of Station 18 because of the three dimensional effects of the actual installation. This latter effect could not be predicted by the simplified axisymmetric model.

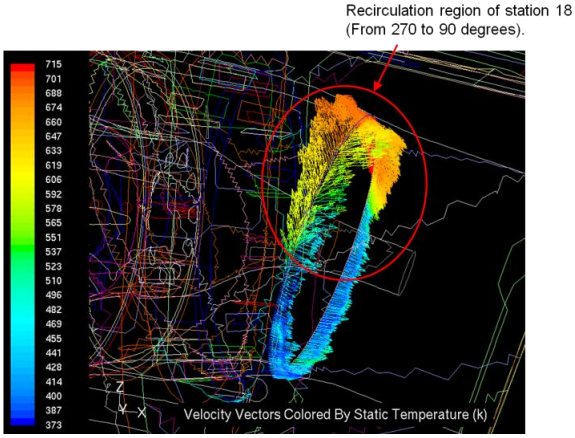

Figure 13: CFD simulation: Reverse flow

3. Solution Identification

Different possible solutions were analyzed:

1. **Nacelle ejectors** (figure 14). Ejector nozzles blow engine bleed air into the exhaust system and suck air from the nacelle bay. This is an effective mean to prevent the reingestion issue, but:
    a. An active system or crew intervention is necessary to control the ejector flow. Active systems may be subject to failure and thus, the operational reliability may be compromised.
    b. Bleeding air from the engine is a penalty in terms of fuel consumption.

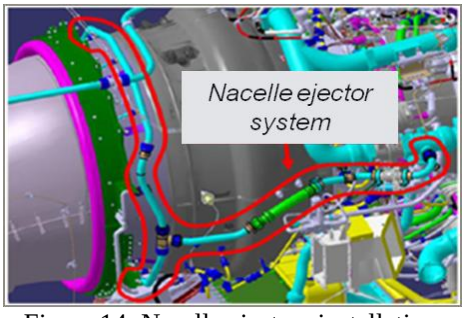

Figure 14: Nacelle ejectors installation

2. **Chevrons** (figure 15). Chevrons are intended to enhance the mixture of engine and ventilation flows, favoring energy transfer from the first to the second flow.

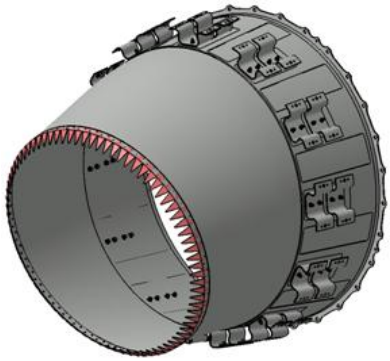

Figure 15: Chevrons on primary nozzle

3. **Local modification of ventilation flow passage** (figure 16). The purpose was to decrease the static pressure at St18, and restrict the onset of reverse flow towards the engine ventilation bay.

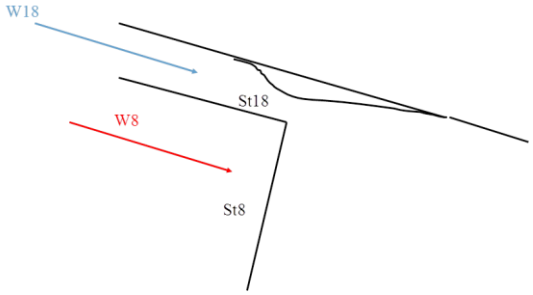

Figure 16: Local modification of ventilation flow passage

4. **Local Flow Conditioners** (LFC-fig 17). LFC devices proved to be the most effective solution to the mentioned problems at minimum cost. This solution avoids the hot air reingestion towards the engine ventilation bay.

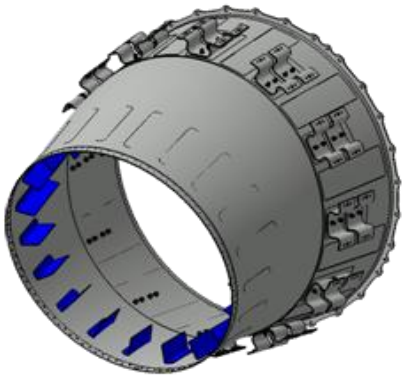

Figure 17: Local Flow Conditioners on the engine nozzle.

The rationale behind the introduction of these devices is explained using a simple eductor configuration like that shown in figure 18.

The idea is to align the LFC to the engine flow direction at conditions for which the engine flow swirl is significantly low, for instance cruise conditions and high power settings (figure 18). Thus the interference of these devices on the engine flow is minimized in power conditions other than idle settings, whereas the LFC will straighten the flow for high swirl conditions.

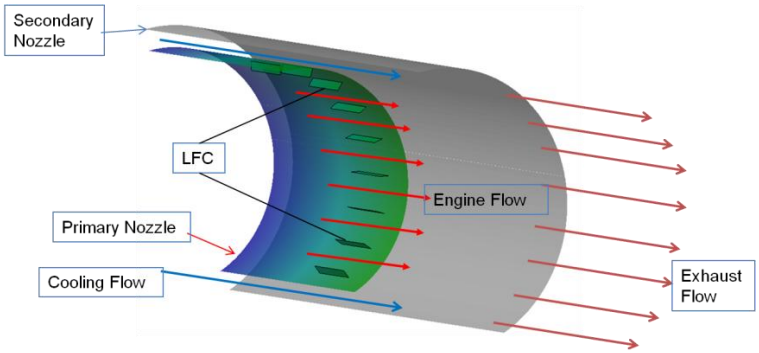

Figure 18: Local Flow Conditioners on the engine nozzle (no swirling flow).

For these conditions LFC devices locally reduce the tangential velocity component. Additionally some secondary vorticity is added on the engine flow, thus favoring the mixture between ventilation and engine flows (figures 19 and 20).

Figure 19: LFC effect on eductor operation (high swirl).

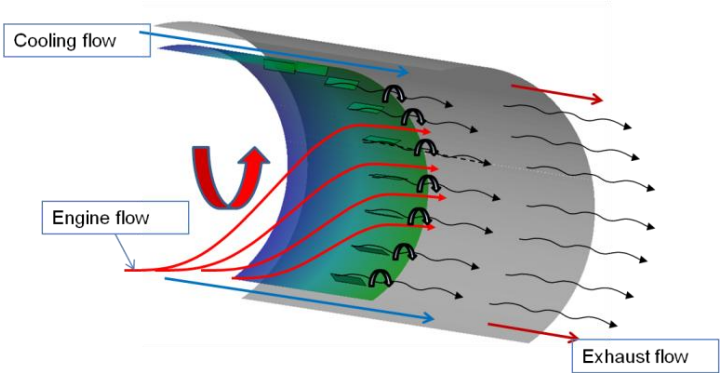

Figure 20: LFC on the engine nozzle (engine swirling flow).

The LFC concept demonstration was accomplished in two steps:

1. Use of CFD analysis allowing for an initial theoretical feasibility of the concept.
2. Flight test.

4. CFD Analysis

In order to show the effect of the LFC devices, a **simplified CFD model** of the actual engine exhaust geometry was used. The purpose of these computations was to prove the effectiveness of the proposed solution before its implementation and test on the actual engine.

The engine exhaust was modelled as three concentric ducts (Figure 21 - Left). One for the engine core flow, other for the ventilation flow coming from the nacelle ventilation bay; and another one, for the flow coming from the OGV refrigeration system. Figure 21 - Right shows the geometry formerly described together with the farfield geometry.

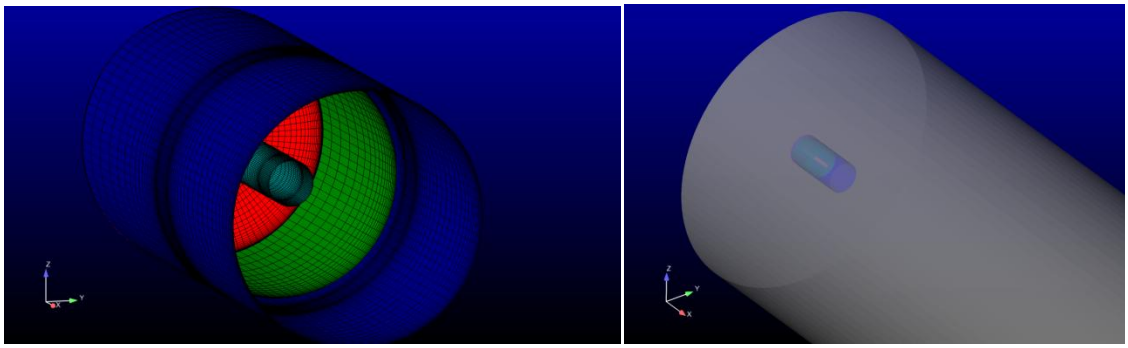

Figure 21. Geometry of the simplified exhaust

Two configurations have been studied with this model:

- Baseline configuration. Eductor without LFC.
- Eductor with LFC.

Since the problem under investigation is periodic, the computational domain was restricted to only one periodic sector. It was meshed with a periodic conformal hexahedral mesh with boundary layer refinement for y^+~1, the total mesh size, irrespective of the configuration, was roughly $1 \cdot 10^6$ nodes. In Figures 22 and 23 the mesh topology for the LFC case and the boundary conditions assignment are shown.

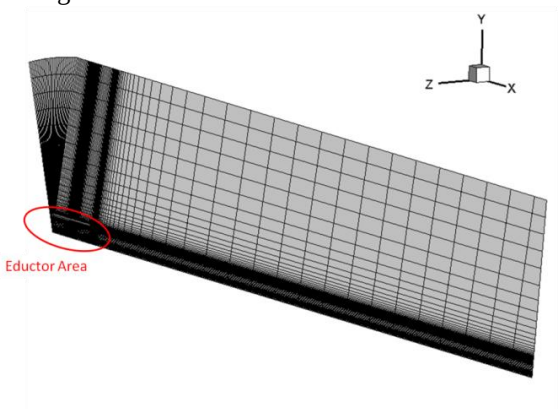

Figure 22.Mesh topology (including far field)

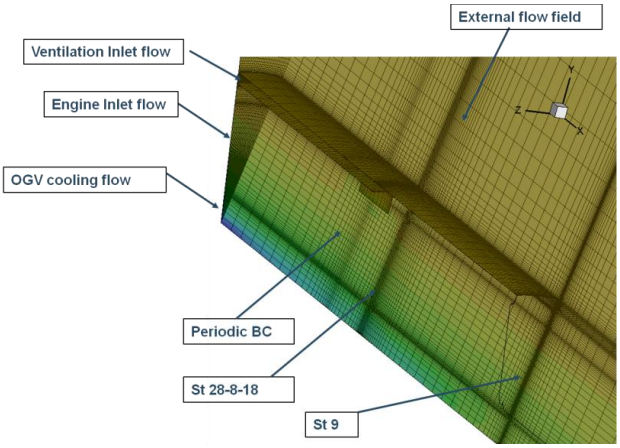

Figure 23.Mesh topology (detail of the eductor area)

The solver used this time, by contrast to the one used for the preliminary CFD studies, was CFX version 11. The spatial derivatives were discretized using a 2nd order accuracy approximation. The air was modeled as an ideal gas and the turbulent model selected was the k-ω SST with the CFX automatic wall functions formulation, which switches from wall functions to low Reynolds formulation treatment when the mesh is fine enough near the wall.

The flight condition investigated was the same Ground Idle engine condition at SL/ISA+40 that was studied during the preliminary CFD phase to identify the source of the problem. The discharge of the exhaust was supposed to be at the atmosphere at rest. The boundary condition imposed at the farfield surfaces was an opening where the static pressure and temperature were fixed. At the engine inlet, the mass flow, the total temperature and the direction of the flow (swirl) were fixed with an inlet boundary condition. The swirl is constant and no radial variation was introduced. As with the preliminary simulation all the former values were obtained from the engine deck. At the Ventilation and the OGV inlets the static temperature and static pressure were fixed with opening boundary conditions. The mass flow at stations ST18 and ST28 are a result of the simulation and thus they are not fixed initially.

In order to assess the effect of the engine swirl on the ventilation performances, CFD simulations for swirl values of 0, 30, 45 and 60 degrees were run.

Figure 24 shows the different ventilation performance between both configurations. All values are referred to ventilation mass flow for the baseline configuration. As it can be seen, as the engine swirl increases, the LFC configuration maintains similar ventilation flows, while for the baseline configuration it collapses. For a swirl value near 60 deg the ventilation flow (ST18) is almost null.

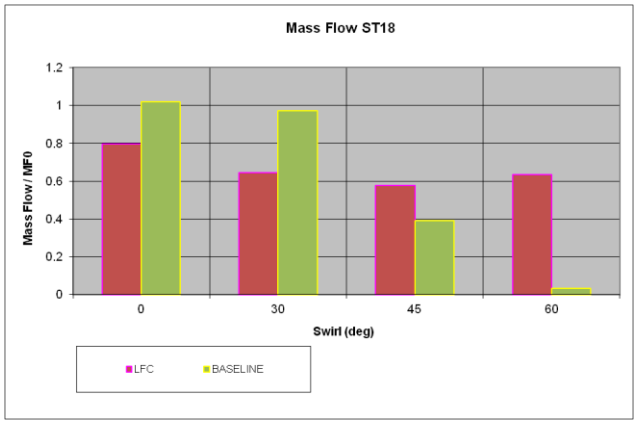

Figure 24.Ventilation mass flow.

Figure 25 and 26 show the static pressure ratio contours at different stations along the exhaust for both configurations, baseline and LFC, respectively. As it can be clearly seen, the effect of the LFC devices is to kill the swirl from the engine and thus significantly reduce the expansion of the engine flow against the secondary exhaust casing, resulting in a higher ventilation flow.

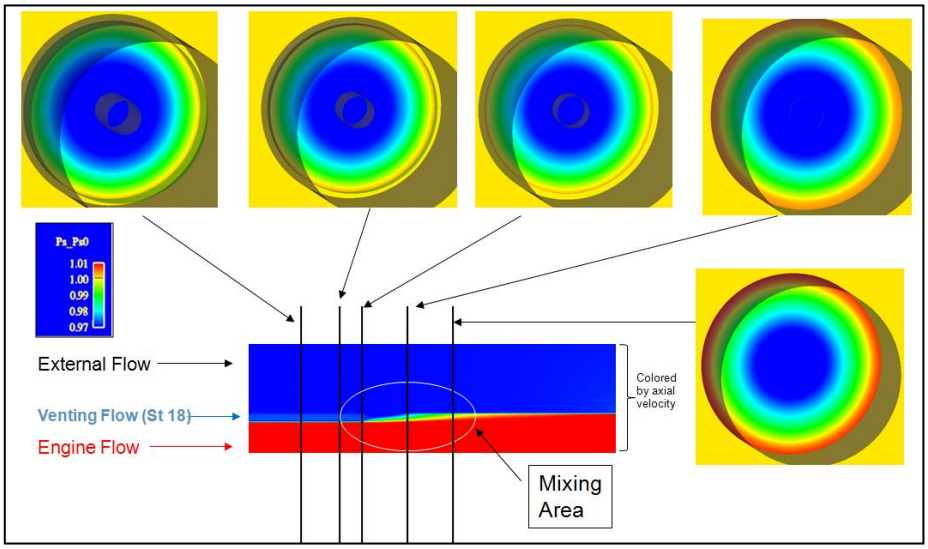

Figure 25. Baseline: Static Pressure ratio contours (GI) Engine Swirl=60º

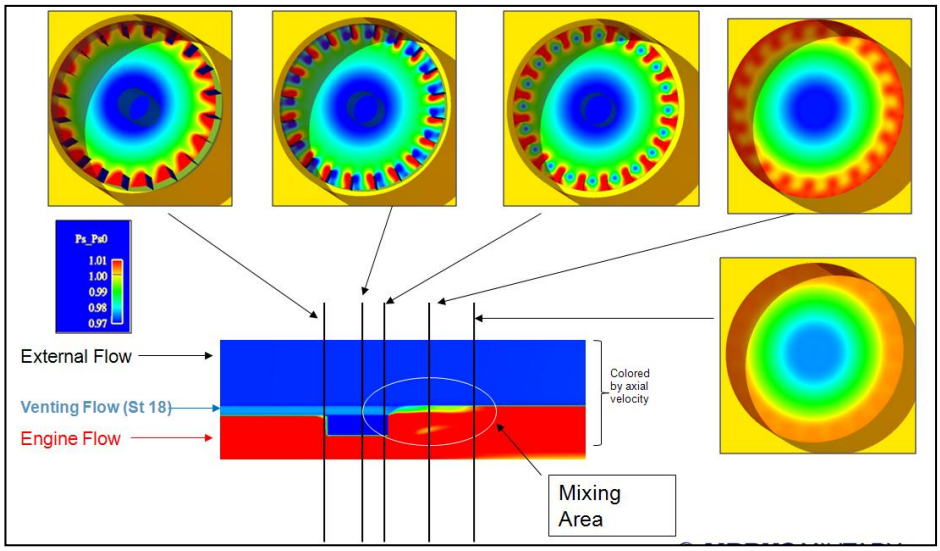

Figure 26. LFC: Static Pressure ratio contours (GI) Engine Swirl=60º

Figure 27 and 28 show the axial velocity contours at different stations along the exhaust for the both configuration, baseline and with LFC, respectively. It can be clearly seen that vorticity that develops due to the separation at the LFC.

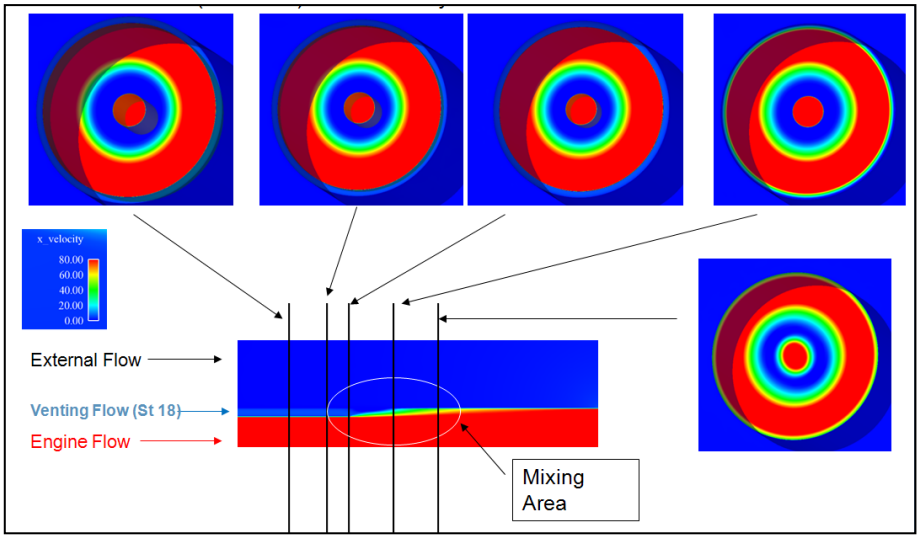

Figure 27. Baseline configuration. Axial velocity contours (GI) Engine Swirl=60º.

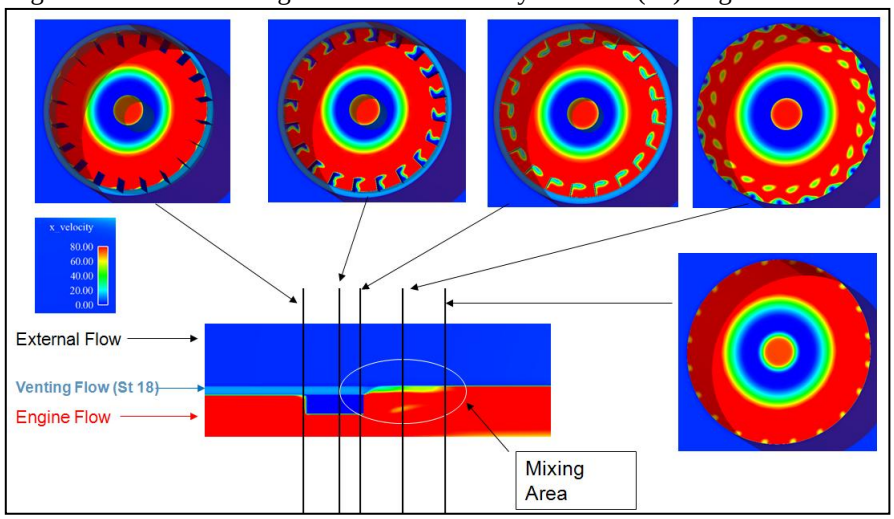

Figure 28. LFC. Axial Velocity contours contours (GI) Engine Swirl=60º

In Figure 29 streamlines near the LFC are shown. The yellow stream lines correspond to the engine flow, while the red stream lines correspond to the ventilation flow. Both images, left and right, only differ in the point of view. One is focused on the core flow while the other is focused on the ventilation flow. It can be seen how the LFC kill the engine swirl and straighten the core flow.

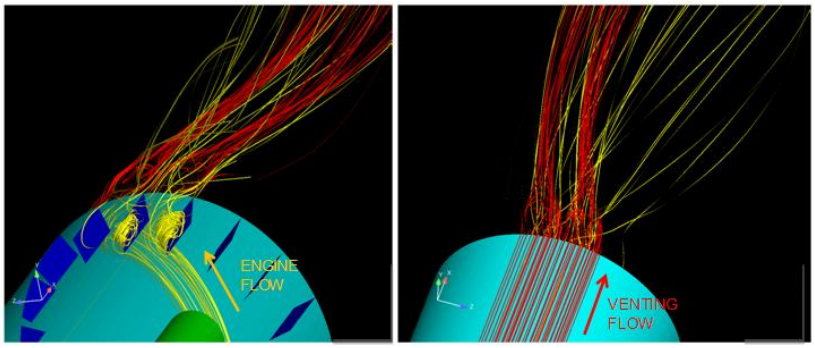

Figure 29. LFC: Streamlines (GI) Engine Swirl=60º.

A similar model was used to assess the effect of chevrons on ventilation. Figure 30 shows how the mixture between engine flow and nacelle ventilation flow was improved, but the engine swirl was not corrected. The result was an inefficient alternative as compared with LFC devices.

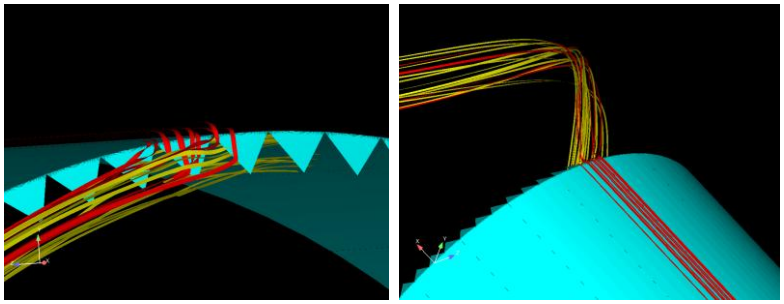

Figure 30. Chevrons: Streamlines (GI) Engine Swirl=60º.

5. Flight Test Results

Once the concept was validated it was installed and flown on a prototype (figure 30). Only one of the engines was equipped with LFC while all the other were kept in the baseline configuration.

Figure 31 shows the effect of the LFC installation on nacelle temperatures. Once the A/C operation is set to Flight Idle, engine ventilation flow temperatures (TT17) start to increase dramatically (engine without LFC), whereas at the ventilation bay which houses the engine equipped with LFC, measured temperatures remain at similar level.

Figure 30. LFC installed on the A/C prototype.

Once the concept was validated it was installed and flown on a prototype (figure 30). Only one of the engines was equipped with LFC while all the other were kept in the baseline configuration.

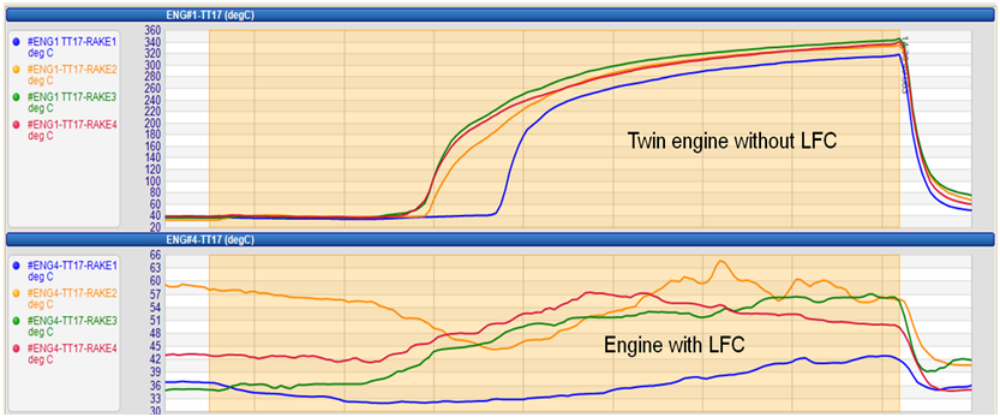

Figure 31 Flight test data: Nacelle ventilation bay temperatures at Flight Idle.

In conclusion: LFC devices are working as expected.

6. Conclusions

The implemented design consisting of a set of fins which locally condition the engine flow have eliminated overheat event of the nacelle ventilation bay. The following design characteristics are met:

- Passive solution.
- Simplicity
- Low cost
- No maintenance required.
- No penalties

Table 1 summarizes the benefits of the installation of the LFC devices versus the conventional solution of installing nacelle ejectors.

Exhaust with nacelle ejectors	**Exhaust with LFC**
Re-ingestion of engine exhaust gases towards the nacelle ventilation bay at low power settings not fully solved with ejectors	Avoiding re-ingestion of engine exhaust gases towards the nacelle ventilation bay
High impact on performances	Low impact on performances
Reliability issues & maintenance needed	Fully reliable & no maintenance
Ejectors: weight impact and cost.	A/C weight saving and cost reduction
Restrictions in the flight envelope (steep descent and low power operations)	No restrictions in the flight envelope (steep descent and low power operations)
Restrictions in ground operations (taxi and Ground Idle)	No restrictions in ground operations (taxi and Ground Idle)

Table 1.Benefits of LFC devices

CFD analysis has been able to provide the proof-of-concept to go ahead with the actual development on A/C hardware. Flight test campaigns have finally proved the validity of the configuration.

The resultant flow evacuation system has been granted the right of European patent No. 11382059.1 2321.

References

[1] Society of Automotive Engineers 1999. Performance of Low Pressure Ratio Ejectors. In: *SAE Aerospace Information Report*. AIR 1191 Rev. A.

[2] European Patent Office 12.09.2012. Flow evacuation system for an aircraft engine. European Patent Application EP 2 497 934 A1